ASEG-PESA 2013
'THE EUREKA MOMENT'
11-14 AUGUST 2013 • MELBOURNE, AUSTRALIA

Correcting for SPM effects in airborne EM

Terence Kratzer
RMIT University
GPO Box 2476
Melbourne VIC 3001
Australia
terence.kratzer@rmit.edu.au

James Macnae
RMIT University
GPO Box 2476
Melbourne VIC 3001
Australia
james.macnae@rmit.edu.au

Paul Mutton
Southern Geoscience Consultants
PO Box 694
Belmont WA 6984
Australia
paul@sgc.com.au

SUMMARY

Recent noise reductions in airborne electromagnetic (AEM) systems have allowed detection of conductors at great depths, but systems now have also become sensitive to superparamagnetic (SPM) effects. We distinguish SPM effects in airborne electromagnetic survey data from the response of good conductors. In electromagnetic data processing, off-time data can be accurately represented as amplitudes of a set of basis functions that are comprised of decays that decrease exponentially as a function of time. The SPM impulse response can be approximated by a decay that is proportional to time to the inverse power, a time dependence associated with magnetic viscosity. We identify the presence of SPM effects, as distinct from the decay of good conductors, by using inverse power-law decays as additional basis functions in constrained least-squares fitting. Application of the method to airborne time-domain electromagnetic (TEM) surveys shows that the method allows correction of SPM and hence aids significantly in conductive target identification.

Key words: airborne EM, magnetic viscosity, SPM, superparamagnetic.

INTRODUCTION

Superparamagnetism (SPM) effects in airborne electromagnetic (AEM) surveys can be a source of needless expense in exploration if not identified, due to unnecessary drilling or further exploration. AEM surveys are commonly used for conductor mapping. Figure 4 shows, for example, the EMFlow apparent conductance (surface to 600 m depth) for a VTEM survey in the Mwese area in Africa. There are many high conductance anomalies on the map that would appear at first glance to be suitable drilling candidates in this dataset. With recent reductions in AEM noise levels, SPM effects (explained in the next section) has become an issue in low-amplitude, late-delay time data, and many anomalies have been drilled based on mistaken interpretation (Mutton, 2012). The challenge lies in determining which of these anomalies indicate basement conductor responses, and which indicate SPM responses.

METHOD AND RESULTS

For a distribution of SPM decays, the signal from SPM appears as proportional to 1/t, in a dB/dt receiver. We use a 1/t basis function, together with exponential decays, to decompose AEM data.

Previous work has described basis function decomposition of AEM data (Macnae et al., 1998) for EM response characterisation. This approach has recently been extended to airborne IP effect detection through least-squares fitting of both EM and IP basis functions as described in Kratzer and Macnae (2012). This last paper provides a comprehensive description of basis function fitting methodology, which we will briefly summarise below. To fit for SPM effects we add a single basis function to the equation representing an inverse delay-time:

$$A^{SPM}(t_k, t_{k+1}) = \frac{1}{2(t_k + t_{k+1})}$$

where t_k and t_{k+1} are the start and end of the sample windows with respect to the primary field turn-off. We then construct our least-squares problem:

$$R = \begin{bmatrix} A^{EM} & A^{IP} & A^{SPM} \\ \Lambda & 0 & 0 \end{bmatrix} \begin{bmatrix} a^{EM} \\ a^{IP} \\ a^{SPM} \end{bmatrix}$$

where R is our time-series data, AEM are our exponential EM basis functions, A^{IP} our IP basis functions, A^{SPM} is our SPM basis function from equation 4, Λ is the smoothing parameter bidiagonal matrix of –λ and λ, and a^{EM}, a^{IP} and a^{SPM} are the EM, IP and SPM amplitudes.

AIP effects in AEM were accurately modelled with AIP as well as AEM basis functions as described by Kratzer and Macnae (2012). In the current work, we found that several modifications were necessary to the AIP fitting process, in order to reliably detect SPM. For example, we found that if any significant weight was given to minimising errors in fitting the early channels (<0.5ms delay) in VTEM, the SPM basis function was not used, and so these early channels were not used in the processing.

We have found that normalisation of the EM decay basis functions is necessary to prevent the large dynamic range of data leading to unstable fitting. This process may have the effect of allowing unstable fits of the very long and very short decays by the fitting algorithm. In order to reduce the incentive of the least- squares fitting algorithm to fit very long EM time constants to SPM signals, we also normalise the EM smoothing matrix Λ (defined above) (along with the EM basis functions). Figure 1 shows an example of data fitting.

In order to quantify the fitting efficacy on real data, we used a line of VTEM data over an area that we also had Magnetic Viscosity Meter (MVM) data (Mutton, 2012). The two lines we will look at here are known as Kapalagulu Test Lines 1 and 2. They are of particular interest because, as well as the MVM data, they both have known real conductors — Test Line 1 has a basement conductor under non-SPM soil, with adjacent SPM, and Test Line 2 has a basement conductor under SPM.

After undergoing the preliminary process described in the previous section for finding an appropriate l (for Test Line 1, l = 7.8, and for Test Line 2, λ = 5.5), we fitted the lines. We then resynthesised the decay curves, stripping out the SPM component, and used EMFlow to produce CDIs of the two test lines.

Figure 2 shows the results of this fitting for Test Line 1. The figure show MVM data, as well as raw CDI (still containing SPM), and the CDI with the fitted SPM component removed.

Although it is apparent that the fitting process is not perfect, overall the results are good, and correlate with known ground-truthed data. The basement conductors remain, and the SPM effect is fairly effectively reduced. The conductor underneath the SPM — presumably the more challenging scenario — in Test Line 2 is successfully retained (not shown here – see Kratzer et al., 2013). It should be noted that the colour scales for conductivity are different for the raw and SPM-removed CDIs. The tendency of finite conductors to be imaged at too great a depth on a CDI is a known artefact of using a 1D approximation to fit the small amplitude data from a 2D or 3D source (Macnae et al., 1998).

The Mwese survey area (Figure 3) contains large amounts of SPM, as well as a few identified basement conductors. Figure 4 shows an image of conductance after fitting and stripping of the SPM component, using EMFlow conductivity mapping, for a small section in the North-West of Figure 3. Good conductors are yellow to red (in both Figures 3 and 4), and SPM in dark hues (Figure 4 only).

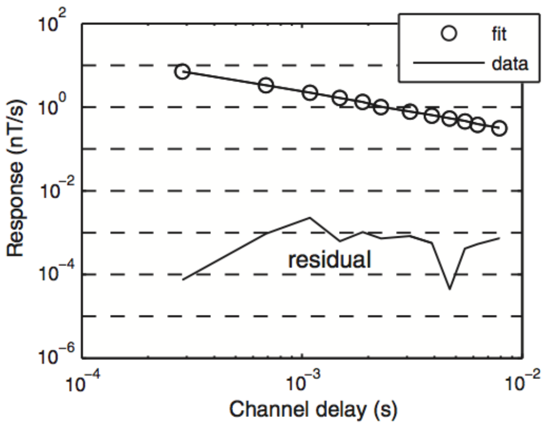

Figure 1. Example of data (circles) and the corresponding fit (line), together with the fit residual, for one particular point (+300 m) of the AMGplate model. This particular point is located over the synthetic SPM, and the fit uses the optimal value of l = 0.02.

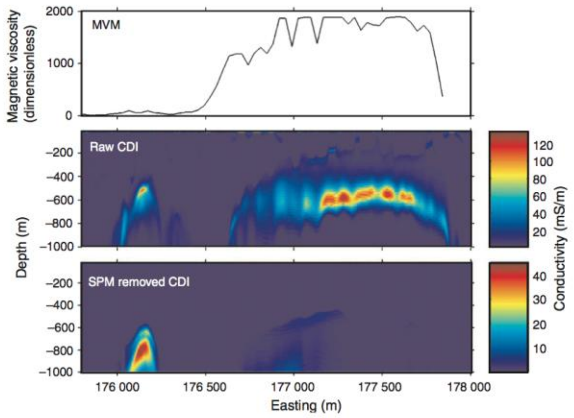

Figure 2. Kapalagulu Test Line 2 (flight 10) results. This line covers a NiS mineralisation (around 178000 m E) under surficial SPM. The area has been ground-truthed for SPM using a MVM (magnetic viscosity meter), and a raw data CDI was produced using EMFlow. Processing using l = 5.5, and subsequent SPM stripping and a re-calculated SPM removed CDI is shown. Note that the true depth of this conductor is ~80 to 100 m.

CONCLUSIONS

We fitted for SPM effects using a t^{-1} basis function, along with other (EM and IP) basis functions in order to provide improved target prioritisation, by indicating where SPM effects are contributing a significant signal. This provides a tool that allows exploration resources to be focused on targets that show the greatest potential to be economic. A major challenge is the basis function matrix stabilisation, and once this has been attained, correctly determining the appropriate value for the smoothing constant λ is difficult and time consuming, but completely necessary for a stable solution. An inappropriate value for λ often leads to instability such that small changes to input data leads to disproportionately large changes in the output.

Some limitations include the fact that we implicitly assume a uniform SPM time constant distribution when we assume a t^{-1} SPM decay. Barsukov and Fainberg (2001) showed that some physical SPM processes can vary by as much as $t^{-1\pm0.2}$, however we have not allowed for this variation. We believe that although allowing for this would further generalise the process, it could also potentially destabilise the fit and produce ‘false positives’ (i.e. indications of SPM effects where there are no SPM effects). Additionally, we have not modified the SPM basis function for primary field shape variation, and we have not corrected SPM signals for height.

The process we have implemented seems to fit SPM when it is present, but it is not infallible. Our opinion is that it appears that it may become a useful tool for target prioritisation.

ACKNOWLEDGMENTS

Thanks to IMX Resources for giving us access to the Mwese and Kapalagulu datasets. Thanks to James Hanneson (Adelaide Mining Geophysics Pty Ltd) for preparing the AMGplate model responses for us. Computing resources for this project came from RMIT University, with support for Terence Kratzer from an Australian Postgraduate Award. James Macnae’s contribution was funded through RMIT University. We thank associate editor Aaron Davis, reviewers

Richard Smith and an anonymous reviewer for their constructive comments on the manuscript.

REFERENCES

Barsukov, P., and Fainberg, E., 2001, Superparamagnetic effect over gold and nickel deposits: *European Journal of Environmental and Engineering Geophysics*, **6**, 61–72.

Billings, S., Pasion, L., Oldenburg, D., and Foley, J., 2003, The influence of magnetic viscosity on electromagnetic sensors: *Proceedings of EUDEM- SCOT2, International Conference on Requirements and Technologies for the Detection, Removal and Neutralization of Landmines and UXO*.

Buselli, G., 1982, The effect of near-surface superparamagnetic material on electromagnetic measurements: *Geophysics*, **47**, 1315–1324. doi:10.1190/1.1441392

Cole, K., and Cole, R., 1941, Dispersion and absorption in dielectrics I. Alternating current characteristics: *The Journal of Chemical Physics*, **9**, 341–351. doi:10.1063/1.1750906

Dunlop, D., and Özdemir, Ö., 2001, *Rock magnetism: fundamentals and frontiers*: Cambridge University Press.

Hanneson, J., 1992, The transient EM step response of a dipping plate in a conductive half space: *Geophysics*, **57**, 1116–1126. doi:10.1190/1.144 3326

Kratzer, T., and Macnae, J. C., 2012, Induced polarization in airborne EM: *Geophysics*, **77**, E317–E327. doi:10.1190/geo2011-0492.1

Kratzer, T., Macnae, J. C., and Mutton, P., 2013, Detection and Correction of SPM effects in airborne EM surveys: *Exploration Geophysics* doi:10.1071/EG12048

Macnae, J., and Lamontagne, Y., 1987, Imaging quasi-layered conductive structures by simple processing of transient electromagnetic data: *Geophysics*, **52**, 545–554. doi:10.1190/1.1442323

Macnae, J., King, A., Stolz, N., Osmakoff, A., and Blaha, A., 1998, Fast AEM data processing and inversion: *Exploration Geophysics*, **29**, 163–169. doi:10.1071/EG998163

Mutton, P., 2012, Superparamagnetic effects in EM surveys for mineral exploration: *ASEG Extended Abstracts*, **2012**, 1–6.

Stacey, F. D., 1963, The physical theory of rock magnetism: *Advances in Physics*, **12**, 45–133. doi:10.1080/00018736300101263

Stanley, J., Sertsrivanit, S., and Clark, P., 1992, Magnetic exploration beneath a near-surface magnetic noise source: *Exploration Geophysics*, **23**, 323–326. doi:10.1071/EG992323

Stolz, E., and Macnae, J., 1998, Evaluating EM waveforms by singular-value decomposition of exponential basis functions: *Geophysics*, **63**, 64–74. doi:10.1190/1.1444328

Watts, A., 1997, Exploring for nickel in the 90's, or 'Til Depth us do Part': *Proceedings of Exploration 97: Fourth Decennial International Conference on Mineral Exploration*, 1003–1014.

West, G., and J. Macnae, 1991, *Physics of the electromagnetic induction exploration method* (volume 2 of Investigations in Geophysics): Society of Exploration Geophysicists.

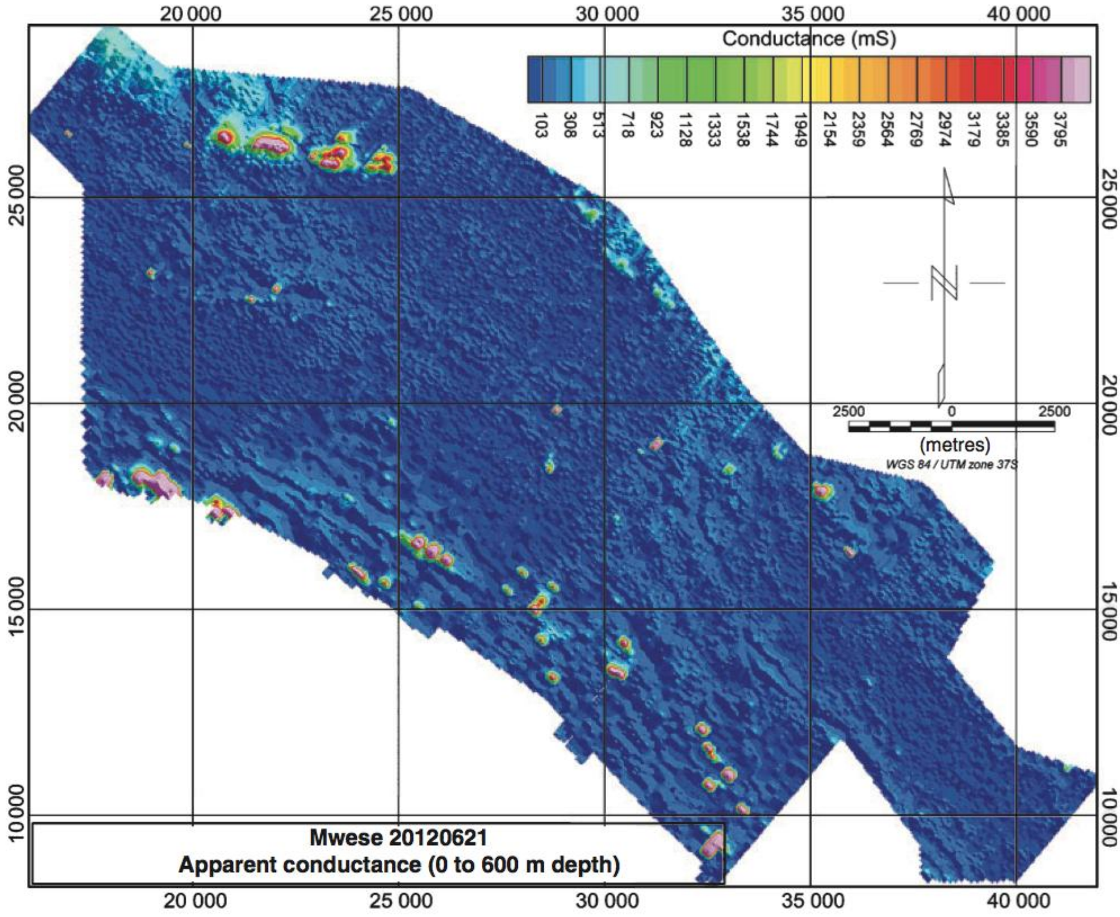

Figure 3. EMFlow apparent conductance map for the Mwese dataset.

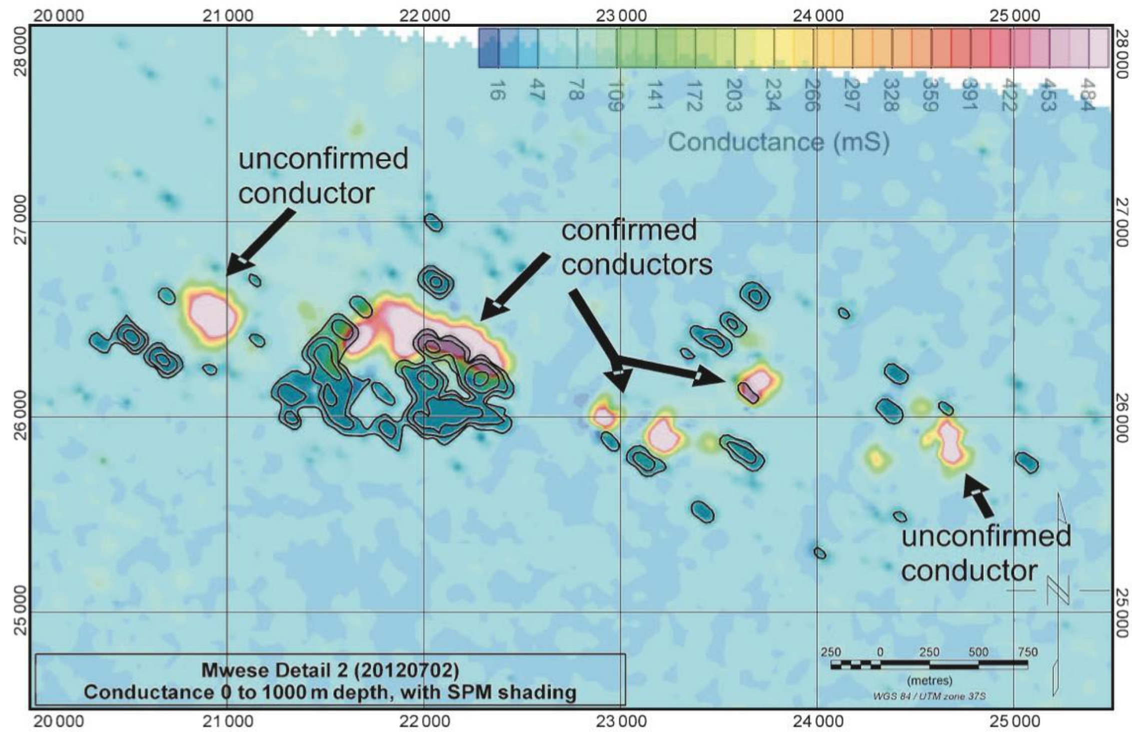

Figure 4. Detail 2 in the Mwese dataset. Areas of detected SPM effects (dark shading and contours) are seen to be displaced from the conductor.